LA-UR-98-1868

Title: Thermal Vaporization and Deposition of Gallium Oxide in Hydrogen

Author(s): Darryl P. Butt, YoungSoo Park, and Thomas N. Taylor

Submitted to: *J. Nucl. Mater.*

Los Alamos NATIONAL LABORATORY

Form No. 836 R5
ST 2629 10/91

submitted to *J. Nucl. Mater.*

Thermal Vaporization and Deposition of Gallium Oxide in Hydrogen

Darryl P. Butt,* Youngsoo Park, and Thomas N. Taylor

Materials Science and Technology Division, Los Alamos National Laboratory, Los Alamos, NM, U.S.A. 87545

Abstract

The thermodynamics of gallium oxide vaporization and deposition in Ar-6% H_2 at elevated temperatures is described. It is shown that Ga_2O_3 vaporizes in H_2 as Ga_2O(g) at elevated temperatures. During thermal processing the Ga_2O(g) moves to cooler zones of the furnace, back reacts with H_2(g) and H_2O(g) and condenses out as Ga(l) and Ga_2O_3(s). Upon removal from the furnace, the exposed Ga forms a ubiquitous surface oxide of Ga_2O_3. X-ray photoelectron spectroscopy (XPS) was used to examine heat treated Ga_2O_3 powders and vaporization products deposited onto SiO_2 and Cu substrates. In agreement with the thermodynamic predictions, these data demonstrate that the deposition product contained Ga_2O_3 and metallic Ga. Analysis of the XPS spectra also revealed an intermediate oxidation state for Ga. The precise bonding of this state could not be demonstrated conclusively, but it is suggested that it may be solid Ga_2O. For coherent product deposition on Cu the metallic Ga concentration increases and the Ga_2O_3 concentration decreases with sputtering depth, suggesting the metallic Ga in the outermost layers of the deposit is readily oxidized during air exposure.

PACS Codes: 73.20, 68.55, 81.15, 81.15
Key Words: gallium, gallium oxide, gallium suboxide, weapons grade plutonium, photoelectron spectroscopy, Auger electron spectroscopy

1. Introduction

There is currently interest in burning weapons-grade plutonium in nuclear reactors, making use of its valuable energy while at the same time reducing certain dangers

* Corresponding author. Tel.: 505-667-9307, e-mail: dbutt@lanl.gov

associated with its potential for nuclear weapons proliferation. In the process of dismantling and declassifying nuclear weapons, the U.S. intends to convert much of the Pu metal to oxide using a hydride-dehydride process.[1] This process yields a PuO_{2-x} powder that potentially can be incorporated into a mixed oxide nuclear fuel, a mixture of PuO_2 and UO_2, or perhaps one day in an advanced non-fertile fuel. However, unlike reactor grade Pu, weapons grade Pu contains minor additions of gallium in order to stabilize the δ-phase, making the alloy easily machinable. Gallium is a known embrittling agent and alloys rapidly with most metals. Consequently, to assure proper cladding and fuel performance, Ga must be largely removed from weapons grade plutonium before it can be processed and used. In order to avoid aqueous processing of this material, which could produce considerable additional waste, we have proceeded toward the development of a relatively simple thermal process for removing gallium from PuO_{2-x} , with the objective of achieving parts per million levels. Our proposed removal process involves heating the oxide in an $Ar\text{-}H_2$ environment, probably at temperatures in excess of 1000°C, producing as the primary gaseous product $Ga_2O(g)$ from decomposition of the Ga_2O_3 present in the mixture. As described below, the equilibrium partial pressure of $Ga_2O(g)$ above Ga_2O_3 is relatively high in a reducing atmosphere. Once evolved, the $Ga_2O(g)$ is swept away from the PuO_{2-x} by the gas stream and must be collected and removed from the heat-treatment system. In this paper, we briefly communicate some of the important fundamentals of the thermodynamics and kinetics of the processes of vaporization and deposition. The primary focus of this paper is on the nature of the deposition product, which is of importance for assessing a means for gallium collection. The deposition products are characterized in detail using X-ray photoelectron spectroscopy (XPS).

2. Thermodynamics of Gallium Oxide Vaporization in Hydrogen

Thermodynamic data for the Ga-O-H system were collected[2-9] and free energies of formation were fit, using stepwise multiple linear regression, to the equation:

$$\Delta G_f = a + bT + cT^{-1} + dT^2 + eT^3 + fT\ln T \qquad (1)$$

where *a-f* are constants, and *T* is temperature in Kelvin. Table 1 shows some of the data pertinent to this brief analysis. Note that other gaseous products such as Ga, GaH, GaO, Ga_2O_2, and Ga_2O_3 are not included in these analyses because their equilibrium partial pressures are comparatively low. The constants in Table 1 were used to calculate temperature dependent expressions for the vaporization behavior of gallium oxide from doped PuO_2 in Ar-6% H_2. A temperature-dependent expression for the free energy of reaction can be determined from the mass-action equation:

$$Ga_2O_3(s) + 2H_2(g) \rightarrow Ga_2O(g) + 2H_2O(g) \qquad (2)$$

From this equation the following relationship was derived from which $Ga_2O(g)$ partial pressures can be calculated:

$$p_{Ga_2O} = \frac{a_{Ga_2O_3} p_{H_2}^2}{p_{H_2O}^2} \exp\left[91.3647 + 1.1203 \cdot 10^{-3} T - 7.761944 \cdot 10^{-8} T^2 - \frac{64223}{T} + \frac{157638}{T^2} - 7.8179 \ln T\right] \qquad (3)$$

Where *a* and *p* represent activity and equilibrium partial pressure, respectively.

Alternatively, the vaporization of $Ga_2O(g)$ may be assessed using the mass-action equation:

$$Ga_2O_3(s) \rightarrow Ga_2O(g) + O_2(g) \qquad (4)$$

where the partial pressure of $Ga_2O(g)$ may be calculated using the equation:

$$p_{Ga_2O} = \frac{a_{Ga_2O_3}}{p_{O_2}} \exp\left[75.69396 - 3.7071 \cdot 10^{-4} T + 2.50277 \cdot 10^{-8} T^2 - \frac{121066}{T} + \frac{117327}{T^2} - 3.82324 \ln T\right] \qquad (5)$$

Equation (5) may be substituted for equation (3) by considering how the partial pressure of oxygen is controlled by the H_2/H_2O ratio according to buffer reaction:

$$H_2(g) + 1/2O_2(g) \rightarrow H_2O(g) \qquad (6)$$

It is apparent from equations (5) and (6) that the higher the H_2/H_2O ratio, the higher will be p_{Ga_2O} (i.e., p_{Ga_2O} is inversely related to p_{O_2}). Thus, the vaporization of Ga_2O would be expected to be more rapid in dry versus moist hydrogen. The equations described above can be used to calculate the equilibrium partial pressures of Ga_2O above various PuO_2-Ga_2O_3 solid solutions. In a typical PuO_2 feedstock, it is anticipated that $a_{Ga_2O_3}$ will be on the order of 0.01 prior to any efforts to remove Ga. However, at this date, the activity of Ga_2O_3 in a typical PuO_2 feedstock powder is not precisely known; therefore, for the purpose of illustration, we must assume certain values of $a_{Ga_2O_3}$. Figure 1, shows how the vaporization behavior varies with environment as a function of $a_{Ga_2O_3}$. The calculations were done assuming the gas was a dry mixture of 1 atm of 6% H_2 and a balance of inert gas, such as Ar or He. This gas composition represents the experimental gases we are using in our Ga removal studies. It is apparent from Fig. 1, that the vaporization rate under the reducing effect of H_2 is relatively high, for example at 1000°C (1273 K) p_{Ga_2O} varies between 10^{-4} and 10^{-2} for $a_{Ga_2O_3}$ between $1 \cdot 10^{-6}$ and 1, respectively. Thus, in a dry hydrogen environment, at elevated temperatures, Ga_2O_3 will vaporize relatively rapidly according to equation (2).

Figure 2 shows the influence of temperature on the calculated equilibrium composition when 1 mole of Ga_2O_3 is reacted with 100 moles of Ar-6% H_2. These complex equilibria were calculated using the computer program SOLGASMIX[10] and available thermodynamic data.[2-9] The possible formation of the condensed phases Ga_2O and $Ga(OH)_3$ was ignored. Figure 2 illustrates that at temperatures greater than 720°C, Ga_2O_3 will react with H_2 forming only $Ga_2O(g)$. Below this temperature, $Ga_2O(g)$ will react with H_2 forming some Ga(l) (note the melting point of Ga is 30°C). Further, it is predicted that some of the Ga_2O(g) will also back react with H_2O(g) forming Ga_2O_3. Thus, we anticipate that in Ar-6% H_2, at elevated temperatures (>720°C) Ga_2O_3 will vaporize to Ga_2O(g). As this gas travels in the gas stream to cooler regions of the furnace, Ga_2O(g) may back react with H_2(g) and H_2O(g) and condense on the furnace walls forming Ga(l) and Ga_2O_3. It should be emphasized that these calculations do not preclude the possible condensation of Ga_2O or $Ga(OH)_3$ species.

3. Experimental Procedures

In order to validate or disprove the deposition process predicted from the aforementioned thermodynamic calculations, Ga_2O_3 powder was placed in the hot zone of a controlled atmosphere furnace. The Ga_2O_3 was 99.999% pure powder (Alfa Aesar, Ward Hill, MA) with the major impurity being 4.0 ppm Sn. Ultra high purity Ar-6% H_2 was flowed through the furnace. The gas was gettered using calcium sulfate and 650°C copper chips to achieve H_2O partial pressures well below 1 ppm. Deposition products were collected near the end of the furnace on either fused SiO_2 or Cu substrates, i.e., inert or reactive substrates, respectively. The deposition products were always a dark, powdery substance. In the case of products deposited onto SiO_2, the residue was carefully removed and mounted as a coherent layer on In foil for analysis. In the case of products deposited onto Cu, the coated substrate was analyzed intact.

The samples were analyzed by XPS in a multitechnique surface analysis apparatus (Model 5600ci, Physical Electronics, Eden Prairie, MN). Spectrometer linearity and absolute energy positions were calibrated to give the Au $4f_{7/2}$, Ag $3d_{5/2}$, and Cu $2p_{3/2}$ peak positions within ± 0.10 eV of 84.00, 368.30, and 932.65 eV binding energy (BE)[11]. Most of the data were taken using unfiltered Mg or Al radiation. One exception to this was the sputter-profiling measurement on the coated Cu substrate, which was done using a monochromatized Al source. Excitation with the Al sources was preferred as it eliminated the strong overlap between the C 1s and Ga LMM transitions. The C 1s peak is important for carbon-based energy referencing. For this reason only data taken with the Al sources are reported herein. The spectra were taken at a pass energy of 23.5 eV to insure high quality peak shapes. During analyses the spectrometer aperture settings were set to allow examination of less than one square millimeter of the sample. Sputter profiling was done in an XPS mode using 4 keV argon ions with a current density of 6 $\mu A/cm^2$ and rastering over a (4x4) mm^2 area. The sputtering rate for these parameters was measured at 15 Å per minute on a reference SiO_2 coating, a value that is taken as the figure of merit for the present work.

The data obtained on the Ga residues were compared with reference spectra acquired from a high-purity Ga_2O_3 powder mounted on In foil. Using this information in conjunction with data found in the literature[12-14] made it possible to interpret the measurements made on the residue. The chief difficulty in analyzing the residues was sample charging under the X-ray source. This was especially true for the materials that had been pressed onto the In foil. Because sample charging uncouples the energy scale of the measured spectrum from the Fermi level of the analyzer, proper interpretation of these spectra requires an internal energy reference or the use of energy differences between appropriate spectral features, the later being independent of the surface potential. Both these methods were used in the data analysis.

In all cases, the C 1s binding energy was used as the internal reference. It was assigned a value of 284.8 eV, which is a generally accepted number for the bonding of adventitious carbon species commonly adsorbed on a surface during air exposure[15]. In comparing the peak positions for several samples, one must assume that the carbon species are equivalent for each case. A better way of differentiating the Ga binding states on these materials is to measure the energy difference between the Ga 3d photoelectron peak and the strongest Ga LMM Auger peak produced by the X-ray radiation. Because of the inequivalence in the electron emission process for these two types of transitions, the difference in the peak energies, known as the Auger parameter[16], is a valid indicator of the

Ga binding state. As excited by a magnesium X-ray source, the published Ga LMM - Ga 3d peak energy differences for metallic Ga and Ga_2O_3 are 167.0 and 170.7 eV, respectively.[13] When acquired using an aluminum X-ray source, these values are shifted to higher energies by 233 eV to 400.0 and 403.7 eV. The peak position for the Ga 3d transition in Ga_2O_3 has been reported at 20.5[12] and 20.8 eV BE[13], while that for metallic Ga is located 1.9 - 2.6 eV lower in binding energy. This information, in combination with our own Ga_2O_3 reference spectra, allowed us to fully interpret the Ga states found on the residue.

4. Experimental Results

Four different deposit and powder samples were pressed onto In foil for analysis. These included: 1) a Ga_2O_3 powder standard, 2) a Ga_2O_3 powder that had been heated to 1100°C in Ar-6% H_2, 3) a black deposition product, scraped from a silica substrate that subsequently had seen hours of air exposure before analysis, and 4) a black deposition product, scraped from a silica substrate that had only seen five minutes of air exposure during transfer to the surface apparatus. Figures 3 and 4 show the Ga 3d and Ga LMM peaks for the above four samples. The kinetic energy values for Fig. 4 were obtained by subtracting the binding energy from the aluminum X-ray energy (1486.6 eV). As shown in Fig. 4, the Auger emission for the single-state Ga_2O_3 reference material exhibits a doublet, whereas the Ga 3d transition in Fig. 3 has a characteristic gaussian-lorentzian shape. In the latter case, the low-level signal intensity above 21.5 eV BE is due to overlap with the O 2s transition. The carbon-referenced peak positions for the Ga 3d and the dominant Ga LMM component are listed in Table 2, along with their energy differences. The Ga_2O_3 reference sample gives an energy difference (403.55 eV) that is 0.15 eV smaller than the value derived from the published literature value[13]. The values from the other samples are no more than 0.45 eV larger. This is a strong indicator that the dominant bonding state is Ga_2O_3 for all the materials. With this in mind and in order to clarify the differences in peak shapes for the powders and deposits on SiO_2 , the spectra for these materials have been plotted with the Ga 3d peak maxima aligned at 19.85 eV BE, the carbon-referenced value for Ga_2O_3 ; consequently, the plotted information is shifted slightly relative to the energy values in Table 2. The vertical lines inscribed on the figures indicate the approximate location of the peaks assigned to the oxide and metallic Ga (or Ga^0) species, consistent with the literature values[12,13].

The Ga LMM spectrum from the deposit loaded with minimum air exposure was simulated using a combination of reference peak shapes for Ga_2O_3, GaO_x, and Ga^0 binding states. The line shapes for each of these states were taken from the Ga_2O_3 reference powder. The three simulation peaks were scaled and their energy shifted to get the best fit to the data, as shown in Fig. 5. There was a significant disparity between the simulation and the data when just two peaks representing Ga_2O_3 and Ga^0 were used in the fit. As indicated by the difference (data minus simulation) plot in Fig. 5, the three-peak simulation did not recreate a continuously flat background in the Ga LMM data. We believe that the three-peak simulation properly reflects the Ga_2O_3 and Ga^0 states, but that the intermediate oxide state or states is less well defined than the approximation used in the fit. Nevertheless, the data give qualitative evidence for an intermediate set of Ga bonding states. For the placement of the Ga 3d data as in Fig. 5, the peak positions for the simulated Ga_2O_3, GaO_x, and Ga^0 states are 423.60, 421.90, and 417.10 eV BE, respectively.

It is possible to better understand the composition of the Ga 3d peak by linking it with the Ga LMM simulation. The aforementioned energy difference for the Ga_2O_3 reference from Table 1 (403.55 eV) was used to define the location of the Ga 3d counterpart. The Ga_2O_3 reference line shape for the Ga 3d transition was then placed at this energy and scaled to give a credible contribution to the Ga 3d data from the deposit, as shown in Fig. 6. A credible contribution was deemed one that, when subtracted from the data, produced a high-binding energy edge on the difference plot that was similar to that seen for the data and reference traces. From the difference plot in Fig. 6 one sees evidence for two states, an intermediate oxide (suboxide) and Ga metal (unoxidized). These two states are located near 19.3 and 17.5 eV BE, respectively. The placement and relative size of the suboxide contribution is heavily dependent on the Ga_2O_3 contribution to the Ga 3d peak, while the metallic peak is less affected. The resultant Ga 3d - Ga LMM energy difference for the metallic Ga is 399.60 eV, which compares well with the published value of 400.00 eV.[13] It is not possible to definitively prove the precise composition of the suboxide state or states, although its Ga 3d intermediate energy position is consistent with previous XPS measurements on condensed Ga_2O.[14]

For the rapidly transferred deposit the energy difference between the primary Ga_2O_3 and Ga^0 contributions in the Ga LMM transition region is 6.5 eV. The same two components with this relative separation are also evident in the spectrum for the deposit with extended air exposure (see Fig. 4). In the latter case, the metallic Ga contribution is noticeably smaller due to the more advanced oxidation in air, which forms an outermost Ga_2O_3 layer. Lastly, the Ga_2O_3 powder that had been heated to 1100°C in argon plus hydrogen only showed a fully stoichiometric oxide configuration (see Fig. 4).

Comparable spectra were obtained from the deposition product on the Cu substrate after it had been exposed to air for about five minutes, as seen in the Ga 3d and Ga LMM data of Figs. 7 and 8. This deposited layer was measured to be 300 Å thick by XPS sputter profiling, which revealed the Cu substrate after 20 minutes of sputtering. The relative positions of the two end-state components in the Ga LMM spectra are near the 6.5 eV separation seen for the Ga_2O_3 and Ga^0 states in the scraped deposit data, described previously. By comparison with the those data, there is clear evidence for metallic Ga, whose contribution relative to the oxide states increases with depth into the material. In view of previous work[17], showing no sputter reduction of Ga_2O_3 by ion bombardment, the Ga chemical state composition should not be affected by the profiling process. The data clearly show that air exposure rapidly oxidizes any metallic Ga component in the topmost layers of the deposit.

5. Concluding Remarks

Thermodynamic calculations of the Ga-O-H system indicate that during high-temperature exposure of Ga_2O_3 to H_2, material will vaporize as predominantly $Ga_2O(g)$. As the gas product is transported to cooler regions of the furnace, the $Ga_2O(g)$ will back react with $H_2(g)$ and $H_2O(g)$ and will condense out as Ga(l) and Ga_2O_3. XPS studies of the deposition product from such a reducing environment generally confirm these thermodynamic calculations.

The XPS data for the deposit scraped from the furnace walls definitely show that the near-surface region is not as fully oxidized when the air exposure is minimized. Furthermore, the relative amount of metallic Ga for the rapidly transferred deposit is larger than that recorded for the as-received deposit on Cu. The larger metallic Ga signal from the former deposit may be ascribed to freshly exposed surfaces of Ga metal, which are produced by the scraping process. For the deposit on Cu the topmost layers of the material are continuously exposed to the reactive gas species in the furnace environment prior to atmospheric exposure.

The increasing amount of metallic Ga observed nearer the Cu interface may represent differences in the thermodynamics of the redistribution in the presence of the Cu oxide on the substrate. However, such an effect may merely be the result of porosity in the deposited layer, where the material deeper in the film is more effectively shielded from the atmosphere, either that of the furnace or during the transfer to the surface apparatus. We can only speculate regarding whether the Ga suboxide indicated by the spectra is more than just a graded oxide layer formed by air exposure. However, it is possible that some of the suboxide is a directly deposited species, in agreement with the Ga_2O known to be produced from thermodynamic considerations.

Acknowledgements

This research was funded under the auspices of the U.S. Department of Energy, Materials Disposition. The authors are grateful for helpful discussions with and the support of John Buksa, David Alberstein, Christopher James and Kenneth Chidester of Los Alamos National Laboratory, and Patrick Rhodes and Jamie Johnson of the Department of Energy.

References

1. T. O. Nelson, M. C. Bronson, D. K. Dennison, B. Flamm, D. Ravenscroft, C. Colmenares, J. Huang, T. Cremers, T. Sampson, L. Bronisz, H. E. Martinez, P. Sayka, D. Pomplun, and R. Hinde, “Advanced Recovery and Integrated Extraction System (ARIES)-Preconceptual Design Report," Los Alamos National Laboratory Report, LA-13178, 1996.

2. I. Barin, *Thermochemical Data of Pure Substances*, VCH Verlagsgesellschaft mbH, New York, 1993.

3. M. W. Chase, Jr., C. A. Davies, J. R. Downey, Jr., D. J. Frurip, R. A. McDonald, and A. N. Syverud, *JANAF Thermochemical Tables*, 3rd Edition, American Institute of Physics, New York, 1986.

4. A. Pajaczkowska and H. Juskowiak, *J. Crystal Growth*, 79 (1986) 421-426.

5. L. M. Foster and J. Scardefield, *J. Electrochem. Soc*., 116 (1969) 494-498.

6. S. A. Shchukarev, G. A. Semenov, and I. A. Rat’kovskii, *Russian J. Inorg. Chem*., 14 (1969) 1-5.

7. C. N. Cochran and L. M. Foster, *J. Electrochem. Soc*., 109 (1962) 146-148.

8. A. U. Seybolt, *J. Electrochem. Soc*., 111 (1964) 697-100.

9. C. J. Frosch and C. D. Thurmond, *J. Phys. Chem*., 66 (1962) 877-878.

10. G. Eriksson, *Chem. Scr*., **8** (1975) 100-103.

submitted to *J. Nucl. Mater.*

11. J. F. Moulder, W. F. Stickle, P. E. Sobol, and K. D. Bomben, *Handbook of X-ray Photoelectron Spectroscopy*, Physical Electronics Division, p. 15, Perkin-Elmer, Eden Prairie, MN (1992).

12. G. Schön, *J. Electron Spec. Related Phenomena*, **2** (1973) 75-86.

13. Y. Mizokawa, H. Iwasaki, R. Nishitani, and S. Nakamura, *J. Electron Spec. Related Phenomena*, **14**, 129-141 (1978).

14. R. Carli and C. L. Bianchi, *Applied Surface Sci.*, **74**, 99-102 (1994).

15. J. F. Moulder, W. F. Stickle, P. E. Sobol, and K. D. Bomben, *Handbook of X-ray Photoelectron Spectroscopy*, Physical Electronics Division, p. 22, Perkin-Elmer, Eden Prairie, MN (1992).

16. C. D. Wagner, L. H. Gale, and R. H. Raymond, *Anal. Chem.*, **51** [4] 466-482 (1979).

17. D. F. Mitchell, G. I. Sproule, and M. J. Graham, *Surf. Interface Anal.*, **15** [8] 487-497 (1990).

List of Figures

from the measured spectrum shows the presence of two additional chemical states, indicated as suboxide and metal.

Figure 7. Ga 3d spectrum from the deposit on Cu as a function of sputtering time. As the Ga_2O_3 enriched surface layer from air exposure is removed, the metallic Ga contribution increases while the oxide persists, indicating that the as-deposited material in the furnace is a mixture of oxide and Ga metal.

Figure 8. Ga LMM spectra from the deposit on Cu as a function of sputtering time. As the Ga_2O_3 enriched surface layer from air exposure is removed, the metallic Ga contribution increases while the oxide persists, indicating that the as-deposited material in the furnace ia a mixture of oxide and Ga metal.

Table 1. Summary of constants shown in equation 1.

Compound	*a*	*b*	*c*	*d*	*e*	*f*
$Ga_2O_3(s)$	-1123572.	574.0020	2267569.	5.3080E-03	-6.8814E-07	-31.7864
$Ga_2O(g)$	-117031.	-55.3176	1295110.	8.3901E-03	-8.9622E-07	0
$H_2O(g)$	-236296.	-65.1431	-169071.	-6.2395E-03	4.2670E-07	16.6059

Table 2. Ga 3d and Ga LMM carbon-referenced peak positions and their binding energy differences for the powders and deposits on SiO_2. See comments in the text regarding energy axis adjustments in the figures.

	Ga 3d	*Ga LMM*		*Peak Difference*
	(eV BE)	(eV BE)	(eV KE)	(eV)
as-received Ga_2O_3	19.85	423.40	1063.20	403.55
heat treated Ga_2O_3	20.20	423.90	1062.70	403.70
deposit, hours in air	20.50	424.50	1062.10	404.00
deposit, minutes in air	20.70	424.40	1062.20	403.70

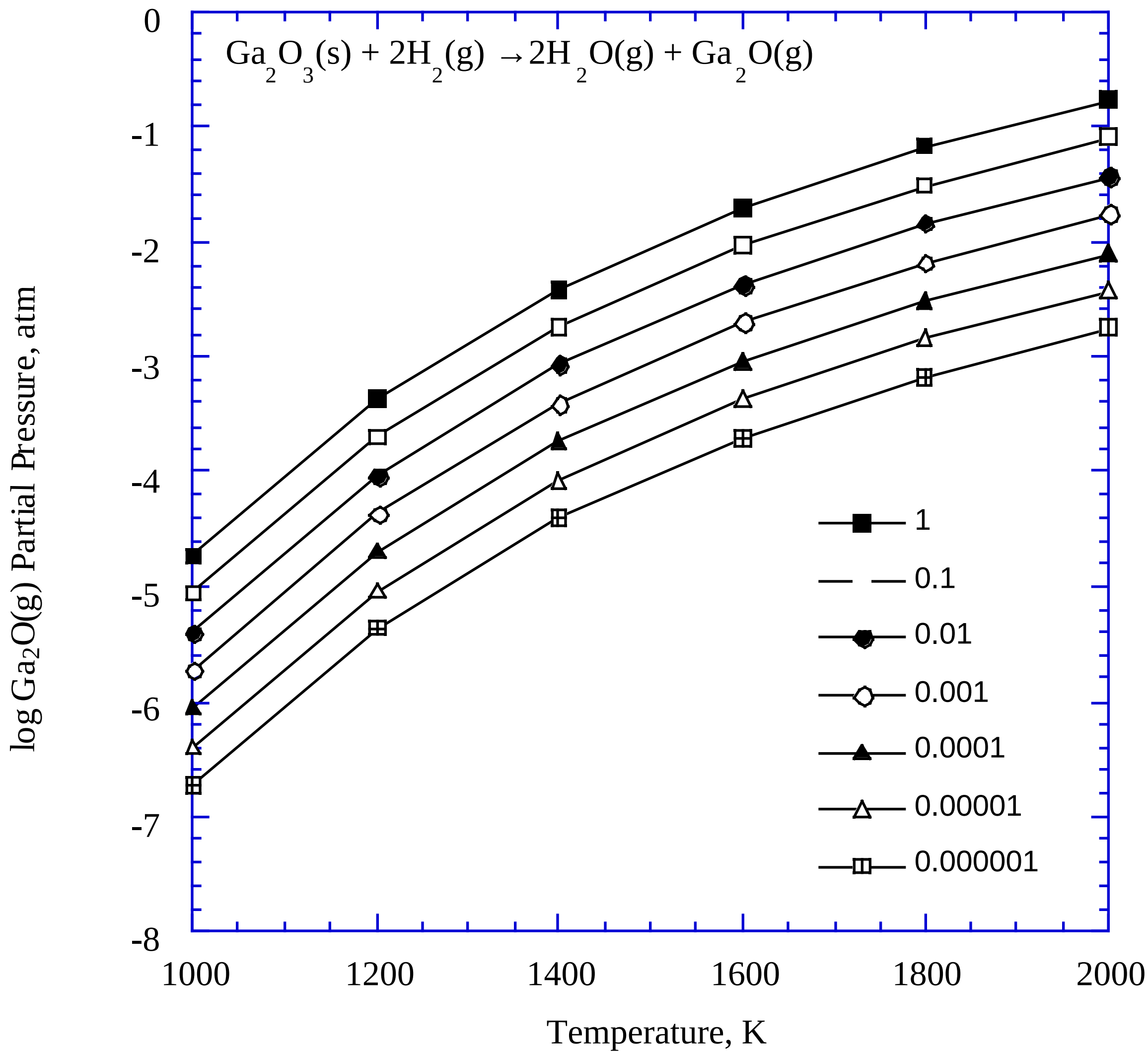

Figure 1. Calculated thermodynamic equilibria of $Ga_2O(g)$ above $Ga_2O_3(s)$ in 0.06 atm of H_2 as a function of temperature and $a_{Ga_2O_3}$. As indicated in the legend, the partial pressures of $Ga_2O(g)$ were calculated for $a_{Ga_2O_3}$ ranging from $1 \cdot 10^{-6}$ to 1.

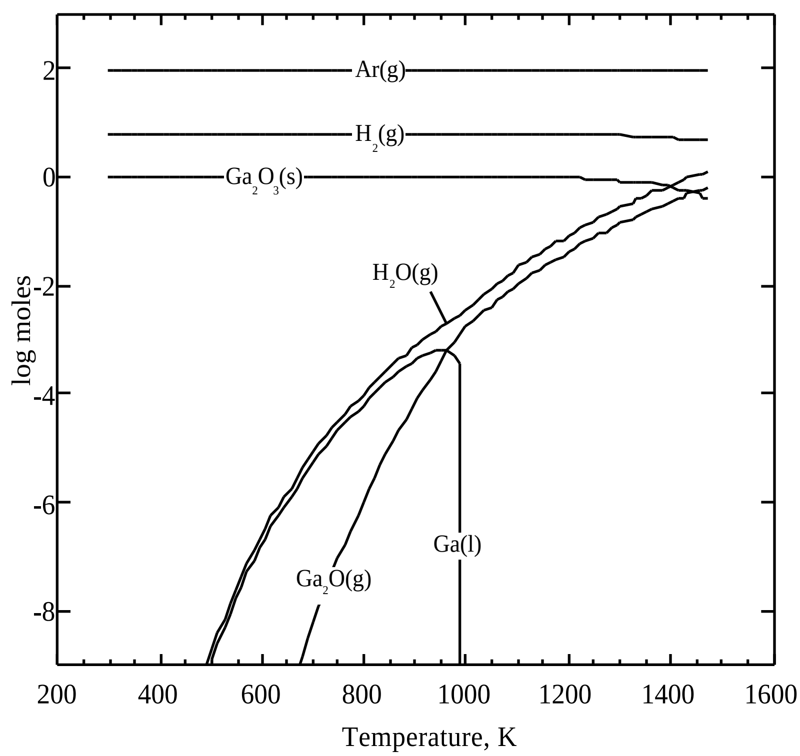

Figure 2. Calculated equilibria at 1 atm between 1 mole of Ga_2O_3 and 100 moles of Ar-6% H_2 as a function of temperature.

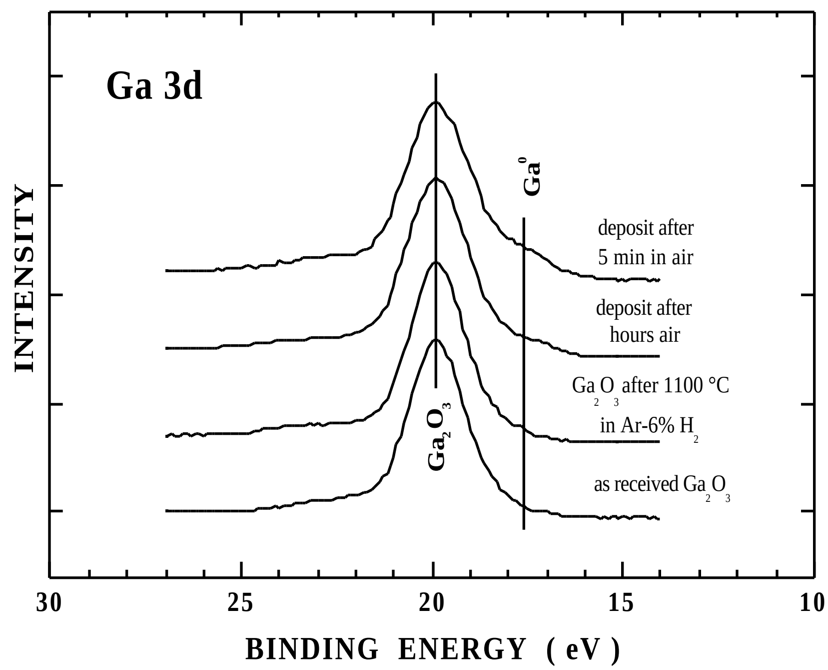

Figure 3. Ga 3d spectra from the as-received Ga_2O_3 powder, the powder after heat treatment in Ar-6% H_2 at 1100°C, and two deposits on SiO_2 (one with hours of air exposure and a second with only minutes of exposure following removal from the heat treatment furnace).

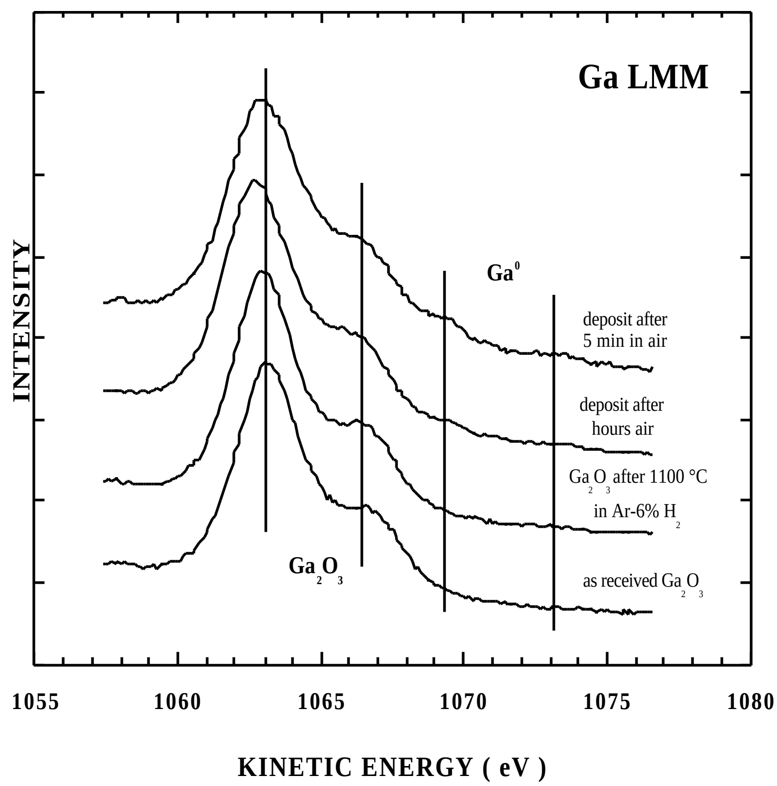

Figure 4. Ga LMM spectra from the as-received Ga_2O_3 powder, the powder after heat treatment in Ar-6% H_2 at 1100°C, and two deposits on SiO_2 (one with hours of air exposure and a second with only minutes of exposure following removal from the heat treatment furnace).

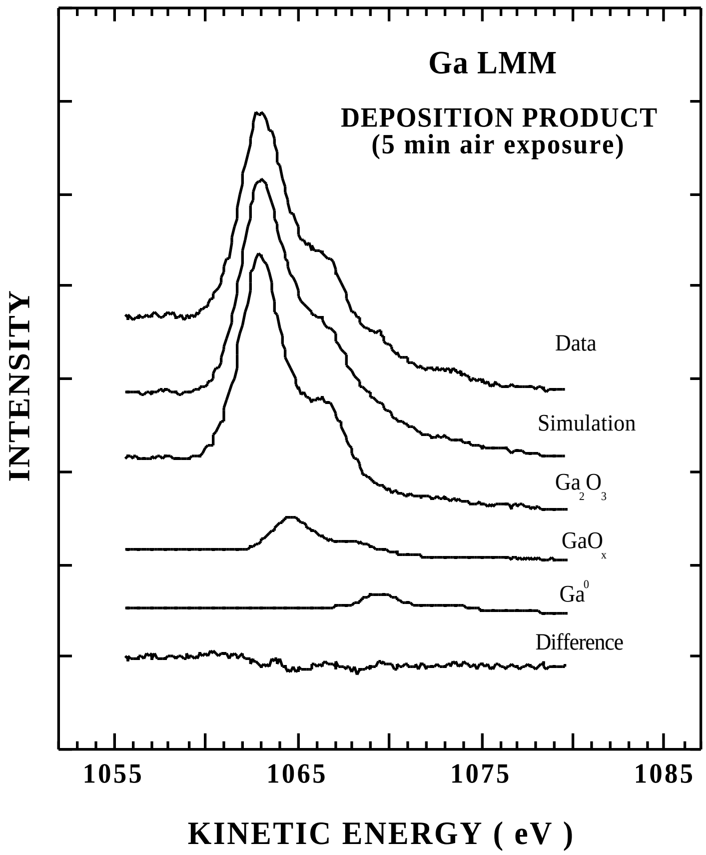

Figure 5. Simulation compared with the measured Ga LMM spectrum from the deposit on SiO_2 (minutes of air exposure following removal from the heat treatment furnace). In addition to the Ga_2O_3 and metallic Ga components used in the simulation, a third contribution (GaO_x) has been introduced that indicates the existence of an intermediate Ga oxidation state (or states). The difference spectrum compares the data with the simulation.

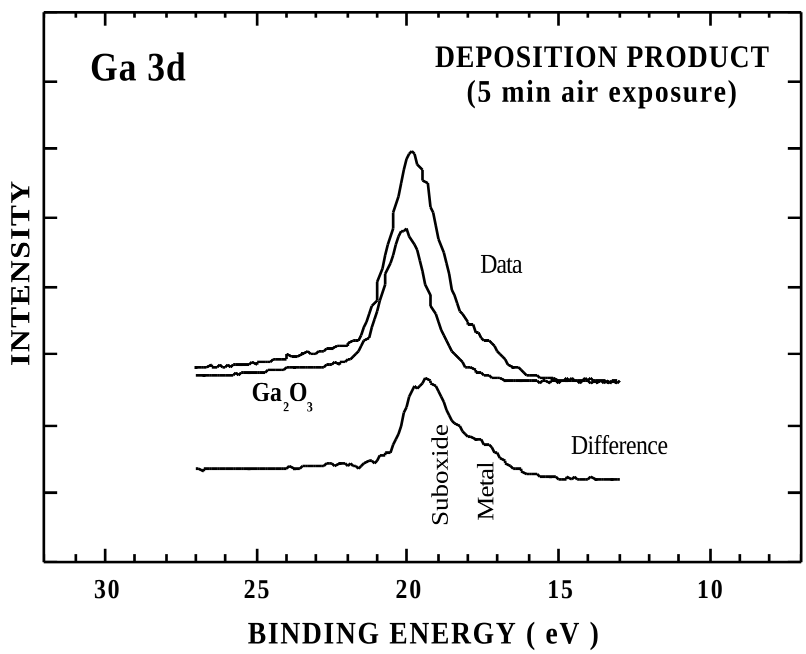

Figure 6. Simulation compared with the measured Ga 3d spectrum from the deposit on SiO_2 (minutes of air exposure following removal from the heat treatment furnace). The Ga_2O_3 component has been positioned relative to its Ga LMM counterpart in Fig. 5 using the energy difference listed in Table 2. Scaling of the Ga_2O_3 component and subtraction from the measured spectrum shows the presence of two additional chemical states, indicated as suboxide and metal.

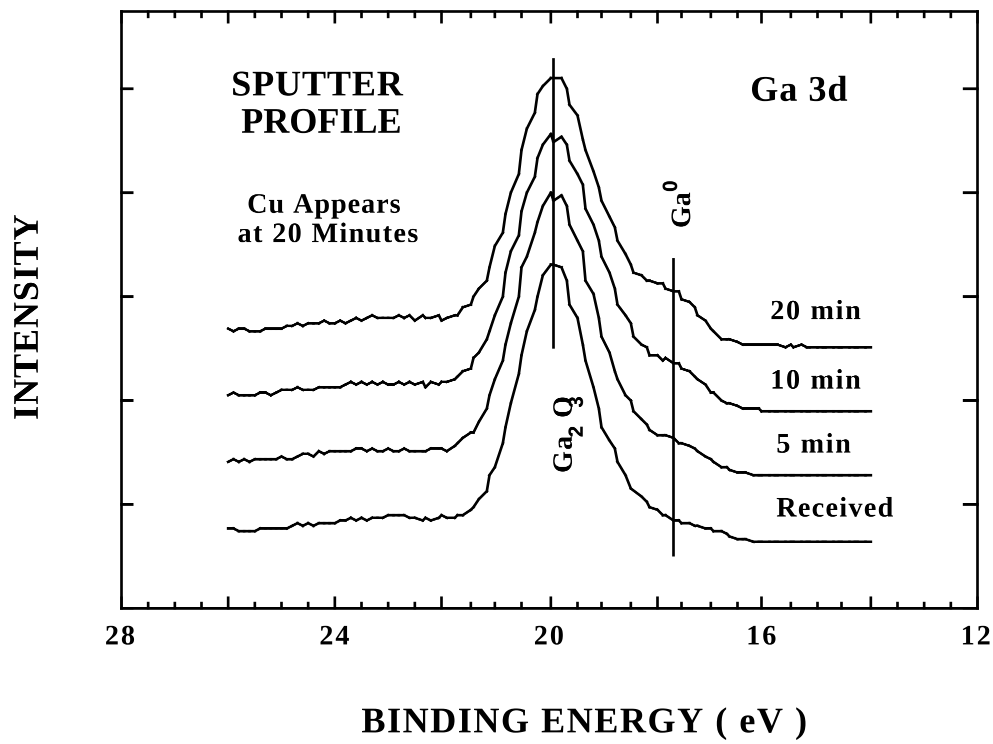

Figure 7. Ga 3d spectrum from the deposit on Cu as a function of sputtering time. As the Ga_2O_3 enriched surface layer from air exposure is removed, the metallic Ga contribution increases while the oxide persists, indicating that the as-deposited material in the furnace is a mixture of oxide and Ga metal.

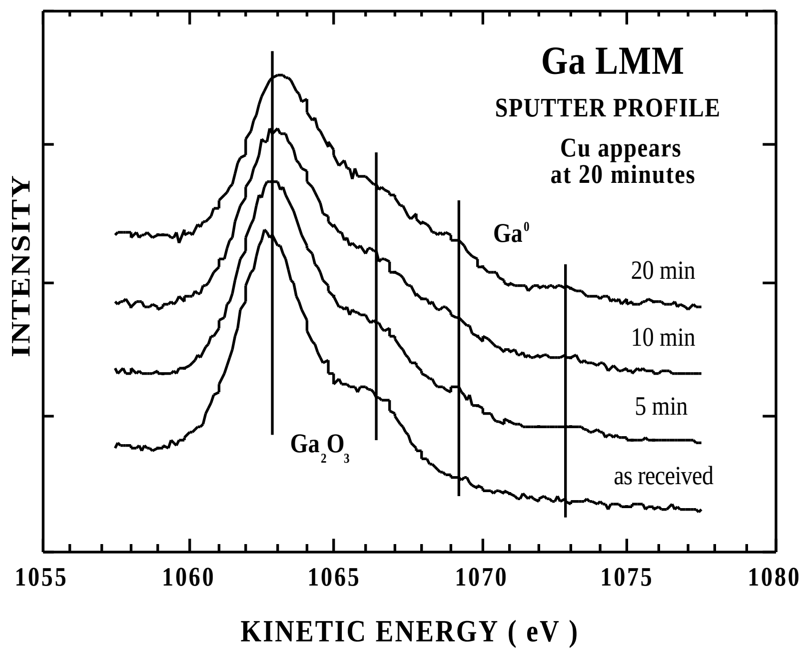

Figure 8. Ga LMM spectra from the deposit on Cu as a function of sputtering time. As the Ga_2O_3 enriched surface layer from air exposure is removed, the metallic Ga contribution increases while the oxide persists, indicating that the as-deposited material in the furnace is a mixture of oxide and Ga metal.